Image Shifting Tracking Leveraging Memristive Devices

Theodoros Panagiotis Chatzinikolaou, Iosif-Angelos Fyrigos, and Georgios Ch. Sirakoulis
Department of Electrical and Computer Engineering, Democritus University of Thrace, Xanthi, Greece

***Abstract*—Unconventional circuits with built-in memory and computing functionalities are becoming the cornerstones of artificial intelligence (AI) at the edge. In the currently deployed systems, sensing and computing occur in separate physical locations, imposing a vast amount of data shuttling between the sensor module and the cloud-computing platforms. Regarding the acceleration of image processing at the edge, in this work, a memristive computing circuit has been designed. By exploiting the non-linear behavior and memory capabilities of memristor devices, a memristive circuit, capable of tracking the shifting of an image is proposed. The presented circuit design can be also combined with an array of sensors, aiming to implement a discrete image tracking module.**

***Index Terms*—In-memory computing, memristive circuit, image processing, edge computing**

I. Introduction

While today's world is characterized by rapid and vivid changes, many new technologies have appeared in the past few years. It is undeniable that the past decade has introduced several tech trends that have become commonplace while still affecting how we live in major ways. From smart driving to elderly fall detection, there are many breathtaking applications that target to enhance the modern lifestyle and to assist in everyday living. The common ground between such applications is usually derived from the computer vision domain where among other processes, the shifting between image frames is required to be tracked.

Autonomous and smart driving has become a top research trend while cars appears to have more advanced sensors than ever. Characteristics like road and lane detection have been introduced and in combination with deep learning they aspire to change the way we drive [1]. Some hardware based neuromorphic proposals have been appeared in literature [2] paving the way of the new autonomous driving era. On the same direction, object detection seems to be a really important task for vehicle and pedestrian detection, as well as in the fields of human–computer interaction and video surveillance [3]. Proposed hardware implementations leveraging novel devices has been also proposed in order to deal with near sensor processing tasks [4].

On the other hand, falling is considered among the most serious hazards to the elderly and, thus, it has piqued the interest of academics and has consistently been one of the most important research topics. Alongside with the technological improvements, falls have been extensively studied by scientific community as it is a hotspot for everyday elderly health-care [5]. Currently, many sensors are used to detect falls, with the sensor-fusion approach being one new trend to increase system performance [6]. However, there is no integrated system to take into account the fall risk and detect falls using camera-assisted observations [7].

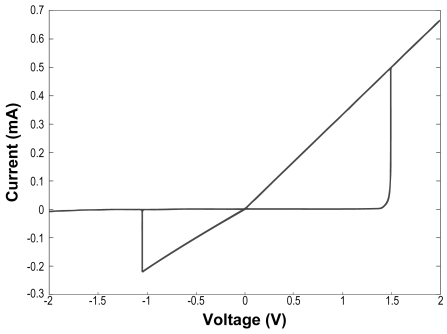

Fig. 1. Stanford memristor model $I - V$ characteristic fitted on fabricated RRAM devices of [8]

Nevertheless, there are many challenges on the way to implement such technologies with the greatest to be the physical limitations. In this context, researchers are attempting to utilize the potential of future and emergent nano-device technologies and unconventional computing approaches inspired by nature in the search for high-density, low-power, high-speed computing systems for the post-CMOS era. Quite recently, a unique nano-device known as the Memristor has been investigated and is considered a viable candidate for significantly improving the processing and storage capacities of developing computer systems. Memristor is a two-terminal nano-scale electronic device that can adapt its electrical conductance in response to the applied voltage on its terminals, while also retaining its conductance value as long as a voltage is not applied, constituting a non volatile memory element [9]. Its potential applications are under investigation, in digital, analog, and mixed signal domains [10]–[19], while it is considered as a good fit for computer vision applications [20]–[22].

There are various memristive approaches for dealing with image processing applications [23], [24]. Expanding the capabilities of memristive systems, in this work, a memristor-based circuit is proposed being able to track the image shifting between two images. Initially, the designed system converts the RGB image input stream to gray-scale, then to binary and finally, through the calculation of various features, determines the direction of image shifting.

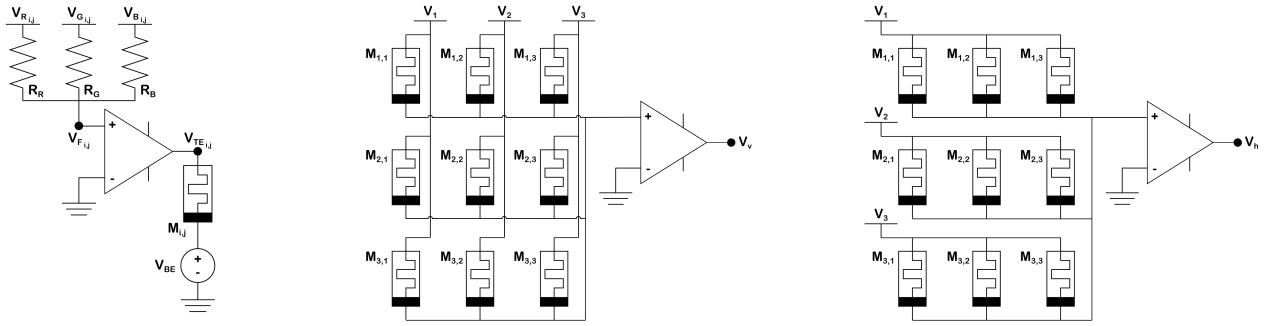

(a) (b) (c)

Fig. 2. (a) Pixel processing system. (b) Vertical and (c) horizontal feature extraction systems

II. Proposed Memristive System

In this Section, the proposed memristive system enabling image shifting tracking is described. As it is expected, three input signals are sent for each pixel of the image; one for red, one for green and one for blue color following the RGB color coding. The voltage values that correspond to the intensity of each color range between 0 and $2.55V$ in order to have an analog equivalent with the digital 8-bit representation of color values, but, more significantly, to supply enough voltage amplitude in order to be able to provoke a change in the resistance of the memristors.

The functionality of the designed memristive circuit can be divided to three operations. Firstly, the designed system converts the RGB image input stream to gray-scale exploiting the Millman's theorem; then by utilizing the memristor non-linear threshold switching dynamics, the image is converted in monochrome. Afterwards, proper input signals are applied to the memristors in order to extract the required features and determine the shifting between two frames.

To design the proposed memristive circuit, the Stanford memristor model has been utilized [25], which has been fitted to fabricated RRAM devices [8]. It is a physics-based RRAM device model with compact equation set, developed in Verilog-A that enables the large scale circuit simulations. The $I-V$ response of the model is presented in Fig. 1. The memristor switches between 3kΩ and 3MΩ resistance with $1.5V$ `SET` and $-1V$ `RESET` threshold, accordingly.

In the proposed RRAM device model the switching is attributed to the formation of a filament which height and width is controlled through the internal variables x and w, respectively. The internal variables equations are the following:

$$dx/dt = af \exp\left(-\left(E - \alpha ZeE\right)/k_B T\right) \tag{1}$$

$$dw/dt = \left(\Delta w + \Delta w^2/2w\right) f \exp\left(-\left(E - \alpha ZeE\right)/k_B T\right) \tag{2}$$

The current of device is calculated through the filament and hopping currents and is provided as follows:

$$I_{CF} = \pi w^2 V_{CF}/4\rho\left(x_0 - x\right) \tag{3}$$

$$I_{hop} = I_0\left(\pi w^2/4\right)\exp\left(-x/x_T\right)\sinh\left(V_{gap}/V_T\right) \tag{4}$$

Further details regarding the model and the corresponding parameters' selection can be examined in [25].

A. Pixel processing

In order to determine the proper weights for each pixel of the image, the input signals should be combined following the Millman's theorem. As each color has different wave lengths and the eye perceives them differently, each color should have a different resistance (R_R, R_G, R_B).

More specifically, the human tri-chromatic color vision is considered for determining the respective resistances as peak sensitivities of each color of different wavelength are not evenly distributed across the visual spectrum [26]. This leads to a better division of red and green colors against other hues.

The respective resistances have been set as follows:

$$R_R = 334\Omega, R_G = 170\Omega, R_B = 877\Omega \tag{5}$$

Thus, this leads to the final weight-averaged signal:

$$\begin{aligned} V_{F_{i,j}} &= \frac{V_{R_{i,j}} \cdot G_R + V_{G_{i,j}} \cdot G_G + V_{B_{i,j}} \cdot G_B}{G_R + G_G + G_B} \\ &= 0.299 \cdot V_{R_{i,j}} + 0.587 \cdot V_{G_{i,j}} + 0.114 \cdot V_{B_{i,j}} \end{aligned} \tag{6}$$

This signal, which corresponds to the gray-scale pixel value, is applied to the top electrode of the memristor via a buffer ($V_{TE_{i,j}}$) to update the weight of the pixel as it can be seen in Fig. 2(a). In order to affect the switching threshold according to the required application, a dynamic DC voltage (V_{BE}) is applied on the bottom electrode of the memristor. This DC voltage provides the system with the ability to tune the sensitivity of the memristors to the gray-scale values. For the correct operation of the proposed application, this voltage has been set to $-100mV$.

More specifically, if $V_{TE_{i,j}}$-V_{BE} is higher than the memristor's `SET` voltage threshold, then the device switches to low resistance state, which corresponds to a white pixel. On the contrary if this voltage is lower, then the memristor remains to high resistance state, corresponding to a black pixel. This processing occurs for every pixel, converting the gray-scale image to a binary one. Consequently, the binary instance of the image is stored in the resistance of the memristors which are arranged in a crossbar-like configuration.

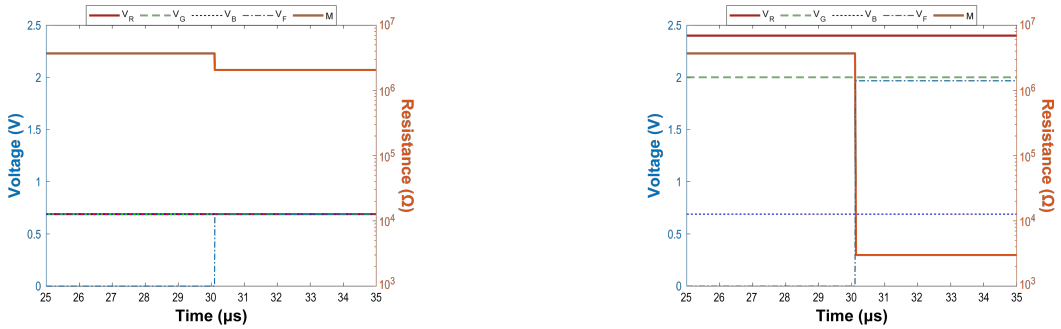

(a) Gray Pixels (b) Yellow Pixels

Fig. 3. Voltage from RGB sources (V_R, V_G, V_B) resulting to different final weight-averaged signals (V_F) and to different memristor resistances (M) during the activation of the pixel processing phase

B. Features extraction

The image shifting takes place in two different axes; i.e., horizontal and vertical. Thus, two different features should be extracted from each image, one for horizontal shifting (V_h) and one for vertical one (V_v). By subtracting these values from one image to another, the pixel shifting can be easily defined.

In order to get these features, the memristors' top electrode is triggered with the respective row or column voltage analogy while the bottom electrode is common for all memristors. The voltage of this common node is considered as the feature's value. The voltage analogy is considered as discrete voltage levels with equally increasing voltage amplitude for each consecutive row or column. Thus, three different voltage levels (V_1, V_2, V_3) are presented in the example of Figs. 2(b,c) to differentiate the three distinct rows or columns, respectively.

Each feature represents in which row or column the white color of the image converges, depicting the weighted average of the white color. Considering that image shifting slightly changes the image position, this leads the white average to get transferred to the corresponding position. By identifying this shifting in both vertical and horizontal axis, the overall image shifting can be determined.

III. Results and Discussion

To evaluate the proper operation of the circuit, a small 3×3 image is considered in Fig. 4(a) for readability reasons. All possible shifting options are considered in Fig. 4(b-i) and the results are presented in Table I. In particular, according to which row or column the yellow pixel is, the respective feature (V_h^i, V_v^i) is settled down to a respective voltage level, i.e. 66.76mV for first, 99.29mV for second and 131.97mV for third one, respectively. Thus, different but discrete voltage differences can be spotted that lead to different shifting levels.

Regarding the operation of the pixel processing procedure, it can be spotted on Fig. 3 for the two different pixel colors of the examples (i.e. gray and yellow). For gray pixel (Fig. 3(a)), the voltages of the respective RGB levels are 0.7V matched to the 8-bit digital equivalent color level of 70. This leads the respective final applied signal to the memristor (V_F) at the same level resulting to an insignificant change to memristor's resistance M. On the contrary, the yellow pixel (Fig. 3(b)) has a red level of 240 and a green of 200 leading to a much higher final weight-averaged voltage of 1.97V after the activation of the pixel processing phase resulting to a significant change of memristor's resistance by 3 orders of magnitude.

The results are following the theoretical background proving the proper operation of the circuit. By examining the image frames in Fig. 4 and the vertical and horizontal shifting values that emerge through the voltage differences of Table I, it can be clearly observed that the circuit calculates correctly the overall shifting of the small image that is proposed here for reference and readability reasons.

IV. Conclusions

In this work, a memristive system is proposed to track the image shifting between different frames. The proposed system processes the input stream of images converting them from RGB to gray-scale, followed by a conversion to binary image by exploiting the non-linear switching dynamics of the memristors. Finally, the stored binary image is utilized to extract and compare the features for horizontal and vertical axis in order to determine the shifting. Examples of all possible shifting combinations have been presented demonstrating the circuit's correct functionality. As future work, memristor variability effect to system performance will be investigated also in terms of area and performance and when compared to similar approaches. Finally, a comprehensive system combined with an image sensor array will be designed focusing on elderly fall, while real data will be analyzed to adjust the system properties for elderly needs.

Acknowledgment

This work has been supported by the project "Study, Design, Development and Implementation of a Holistic System for Upgrading the Quality of Life and Activity of the Elderly" (MIS 5047294) which is implemented under the Action "Support for Regional Excellence", funded by the Operational Programme "Competitiveness, Entrepreneurship and Innovation" (NSRF 2014-2020) and co-financed by Greece and the European Union (European Regional Development Fund).

References

[1] L. Liu, S. Lu, R. Zhong, B. Wu, Y. Yao, Q. Zhang, and W. Shi, "Computing systems for autonomous driving: State of the art and challenges," *IEEE Internet of Things Journal*, vol. 8, no. 8, pp. 6469–6486, April 2021.

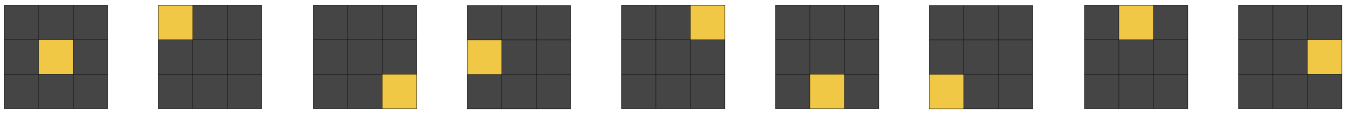

(a) Initial (b) Frame 1 (c) Frame 2 (d) Frame 3 (e) Frame 4 (f) Frame 5 (g) Frame 6 (h) Frame 7 (i) Frame 8

Fig. 4. Initial and following frames visual representation

TABLE I
FEATURES EXTRACTION FOR EACH FRAME

Frame	**Features**		**Difference from Initial**		**Shifting from Initial**		**Difference from Previous**		**Shifting from Previous**	
	V_h^i	V_v^i	$V_h^i - V_h^0$	$V_v^i - V_v^0$	**Vertical**	**Horizontal**	$V_h^i - V_h^{i-1}$	$V_v^i - V_v^{i-1}$	**Vertical**	**Horizontal**
Initial	$99.29\ mV$	$99.29\ mV$	-	-	-	-	-	-	-	-
Frame 1	$66.76\ mV$	$66.76\ mV$	$-32.53\ mV$	$-32.53\ mV$	-1	-1	$-32.53\ mV$	$-32.53\ mV$	-1	-1
Frame 2	$131.97\ mV$	$131.97\ mV$	$32.68\ mV$	$32.68\ mV$	+1	+1	$65.21\ mV$	$65.21\ mV$	+2	+2
Frame 3	$99.29\ mV$	$66.76\ mV$	$0\ mV$	$-32.53\ mV$	0	-1	$-32.68\ mV$	$-65.21\ mV$	-1	-2
Frame 4	$66.76\ mV$	$131.97\ mV$	$-32.53\ mV$	$32.68\ mV$	-1	+1	$-32.53\ mV$	$65.21\ mV$	-1	+2
Frame 5	$131.97\ mV$	$99.29\ mV$	$32.68\ mV$	$0\ mV$	+1	0	$65.21\ mV$	$-32.68\ mV$	+2	-1
Frame 6	$131.97\ mV$	$66.76\ mV$	$32.68\ mV$	$-32.53\ mV$	+1	-1	$0\ mV$	$-32.53\ mV$	0	-1
Frame 7	$66.76\ mV$	$99.29\ mV$	$-32.53\ mV$	$0\ mV$	-1	0	$-65.21\ mV$	$32.53\ mV$	-2	+1
Frame 8	$99.29\ mV$	$131.97\ mV$	$0\ mV$	$32.68\ mV$	0	+1	$32.53\ mV$	$32.68\ mV$	+1	+1

[2] C. Wang, Z. Yang, S. Wang, P. Wang, C.-Y. Wang, C. Pan, B. Cheng, S.-J. Liang, and F. Miao, "A braitenberg vehicle based on memristive neuromorphic circuits," *Advanced Intelligent Systems*, vol. 2, no. 1, p. 1900103, 2020.

[3] Y. Zhang, T. Wang, K. Liu, B. Zhang, and L. Chen, "Recent advances of single-object tracking methods: A brief survey," *Neurocomputing*, vol. 455, pp. 1–11, 2021.

[4] N. Dastanova, S. Duisenbay, O. Krestinskaya, and A. P. James, "Bit-plane extracted moving-object detection using memristive crossbar-cam arrays for edge computing image devices," *IEEE Access*, vol. 6, pp. 18 954–18 966, 2018.

[5] L. Ren and Y. Peng, "Research of fall detection and fall prevention technologies: A systematic review," *IEEE Access*, vol. 7, pp. 77 702–77 722, 2019.

[6] A. Singh, S. U. Rehman, S. Yongchareon, and P. H. J. Chong, "Sensor technologies for fall detection systems: A review," *IEEE Sensors Journal*, vol. 20, no. 13, pp. 6889–6919, July 2020.

[7] A. Ramachandran and A. Karuppiah, "A survey on recent advances in wearable fall detection systems," *BioMed research international*, vol. 2020, 2020.

[8] P. Huang, X. Liu, W. Li, Y. Deng, B. Chen, Y. Lu, B. Gao, L. Zeng, K. Wei, G. Du *et al.*, "A physical based analytic model of rram operation for circuit simulation," in *2012 International Electron Devices Meeting*. IEEE, 2012, pp. 26–6.

[9] L. Chua, "Memristor-the missing circuit element," *IEEE Transactions on Circuit Theory*, vol. 18, no. 5, pp. 507–519, September 1971.

[10] Y. V. Pershin and M. Di Ventra, "Practical approach to programmable analog circuits with memristors," *IEEE Transactions on Circuits and Systems I: Regular Papers*, vol. 57, no. 8, pp. 1857–1864, 2010.

[11] R. Tetzlaff, *Memristors and Memristive Systems*. Springer, 2013.

[12] G. Papandroulidakis, I. Vourkas, N. Vasileiadis, and G. C. Sirakoulis, "Boolean logic operations and computing circuits based on memristors," *IEEE Transactions on Circuits and Systems II: Express Briefs*, vol. 61, no. 12, pp. 972–976, 2014.

[13] L. Chua, G. C. Sirakoulis, and A. Adamatzky, *Handbook of Memristor Networks*. Springer International Publishing, 2019.

[14] I.-A. Fyrigos, V. Ntinas, G. C. Sirakoulis, A. Adamatzky, V. Erokhin, and A. Rubio, "Wave computing with passive memristive networks," in *2019 IEEE International Symposium on Circuits and Systems (ISCAS)*, 2019, pp. 1–5.

[15] T. P. Chatzinikolaou, I.-A. Fyrigos, R.-E. Karamani, V. Ntinas, G. Dimitrakopoulos, S. Cotofana, and G. C. Sirakoulis, "Memristive oscillatory circuits for resolution of NP-complete logic puzzles: Sudoku case," in *2020 IEEE International Symposium on Circuits and Systems (ISCAS)*. IEEE, 2020, pp. 1–5.

[16] I.-A. Fyrigos, V. Ntinas, M.-A. Tsompanas, S. Kitsios, G. C. Sirakoulis, D. Tsoukalas, and A. Adamatzky, "Implementation and optimization of chemical logic gates using memristive cellular automata," in *2020 European Conference on Circuit Theory and Design (ECCTD)*, 2020, pp. 1–6.

[17] T. P. Chatzinikolaou, I.-A. Fyrigos, V. Ntinas, S. Kitsios, P. Bousoulas, M.-A. Tsompanas, D. Tsoukalas, and G. C. Sirakoulis, "Memristive oscillatory networks for computing: The chemical wave propagation paradigm," in *2021 17th International Workshop on Cellular Nanoscale Networks and their Applications (CNNA)*, 2021, pp. 1–5.

[18] T. P. Chatzinikolaou, I.-A. Fyrigos, V. Ntinas, S. Kitsios, P. Bousoulas, M.-A. Tsompanas, D. Tsoukalas, A. Adamatzky, and G. C. Sirakoulis, "Margolus chemical wave logic gate with memristive oscillatory networks," in *2021 28th IEEE International Conference on Electronics, Circuits, and Systems (ICECS)*, 2021, pp. 1–6.

[19] T. P. Chatzinikolaou, I.-A. Fyrigos, V. Ntinas, S. Kitsios, P. Bousoulas, M.-A. Tsompanas, D. Tsoukalas, and G. C. Sirakoulis, "Unconventional logic on memristor-based oscillatory medium," in *2021 10th International Conference on Modern Circuits and Systems Technologies (MOCAST)*, 2021, pp. 1–4.

[20] N. Vasileiadis, V. Ntinas, G. C. Sirakoulis, and P. Dimitrakis, "In-memory-computing realization with a photodiode/memristor based vision sensor," *Materials*, vol. 14, no. 18, 2021.

[21] R.-E. Karamani, I.-A. Fyrigos, K.-A. Tsakalos, V. Ntinas, M.-A. Tsompanas, and G. C. Sirakoulis, "Memristive learning cellular automata for edge detection," *Chaos, Solitons & Fractals*, vol. 145, p. 110700, 2021.

[22] N. Vasileiadis, V. Ntinas, I.-A. Fyrigos, R.-E. Karamani, V. Ioannou-Sougleridis, P. Normand, I. Karafyllidis, G. C. Sirakoulis, and P. Dimitrakis, "A new 1P1R image sensor with in-memory computing properties based on silicon nitride devices," in *2021 IEEE International Symposium on Circuits and Systems (ISCAS)*, 2021, pp. 1–5.

[23] X. Hu, S. Duan, L. Wang, and X. Liao, "Memristive crossbar array with applications in image processing," *Science China Information Sciences*, vol. 55, no. 2, pp. 461–472, 2012.

[24] A. K. Maan, D. S. Kumar, S. Sugathan, and A. P. James, "Memristive threshold logic circuit design of fast moving object detection," *IEEE Transactions on Very Large Scale Integration (VLSI) Systems*, vol. 23, no. 10, pp. 2337–2341, 2015.

[25] H. Li, P. Huang, B. Gao, B. Chen, X. Liu, and J. Kang, "A spice model of resistive random access memory for large-scale memory array simulation," *IEEE Electron Device Letters*, vol. 35, no. 2, pp. 211–213, 2013.

[26] C. Hiramatsu, A. D. Melin, W. L. Allen, C. Dubuc, and J. P. Higham, "Experimental evidence that primate trichromacy is well suited for detecting primate social colour signals," *Proceedings of the Royal Society B: Biological Sciences*, vol. 284, no. 1856, p. 20162458, 2017.